Supplementary material

Topology Analysis Reveals Supramolecular Organisation of 96 Large Independent Complex Ions into one Geometrical Object

Morsy Abu-Youssef, Saied Solieman, Mona Sharaf, Jörg Albering, and Lars Öhrström

Contents:

*1. Comment and analysis of Russo, J., Romano, F., Tanaka, H., New metastable form of ice and its role in the homogeneous crystallization of water, Nat Mater **2014**, 13, 733-739*[1].

We do not want to distract from the qualities of this interesting article merely point out that the network topology approach had been a useful addition to this work.

Russo et al. correctly identities their phase "ice 0" as having the same structure as the T12 group 14 allotrope of Zhao, Z. et al.[2] (Tetragonal allotrope of group 14 elements. J. Am. Chem. Soc. 134, 12362–12365 (2012)). The important point is that these structures both have the **cdp** topology or the same network topology as CdP_2 (incidentally this compound has the same average number of valence electrons as the group 14 elements). Below **cdp** topology from ref. 8.[3] in this article (Öhrström, L., O'Keeffe, M., Network topology approach to new allotropes of the group 14 elements, Z. Krist. Cryst. Mat. 2013, 228, 343-346.) is illustrated. The topology of Ice 0 was verified with the SYSTRE program[4](Identification and symmetry computation for crystal nets. O. Delgado-Friedrichs, M. O'Keeffe, Acta Crystallogr. A 59 351-360 (2003).)

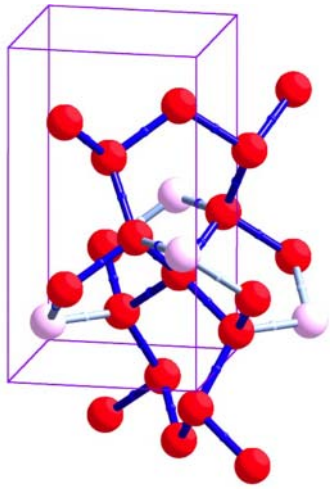

*Figure S1. Left: **cdp** topology from Öhrström and O'Keeffe.*

Russo et al. also correctly identifies (in the supplementary material) the shortest rings as a way of discerning different topologies. Thee sequences are known as "point symbols",[5] and can easily be derived from the "vertex symbols" tabulated in the Reticular Chemistry Structure Resource[6] (http://rcsr.anu.edu.au/). For **cdp** the vertex symbols gives 5.5.5.5.6.6 and 5.6.5.6.5.7(2).

For en earlier comment on the network topology of ice, especially the remarkable ice-XII, see O'Keeffe, M. New ice outdoes related nets in smallest ring size. *Nature* 392 (1998) 879.[7]

We suggest using the network topologies as an additional descriptor for the ice polymorphs as this will make them easier to compare and relate to other compounds, but also for the convenience of the researchers in this particular field.

*2. Hirshfeld surfaces of **1**.*

Hirshfeld surfaces were used to create overall pictures of closest intermolecular atom-atom distances, and specific overviews of C…H and H…H interactions, and these have been depicted in Figure S2. There is some C…H at the flat surfaces and significant H…H interactions between the ends (-CH_2-CH_2- embraces). C…C interactions are insignificant, typically in the range of 0.2% of the surface of each coordination entity

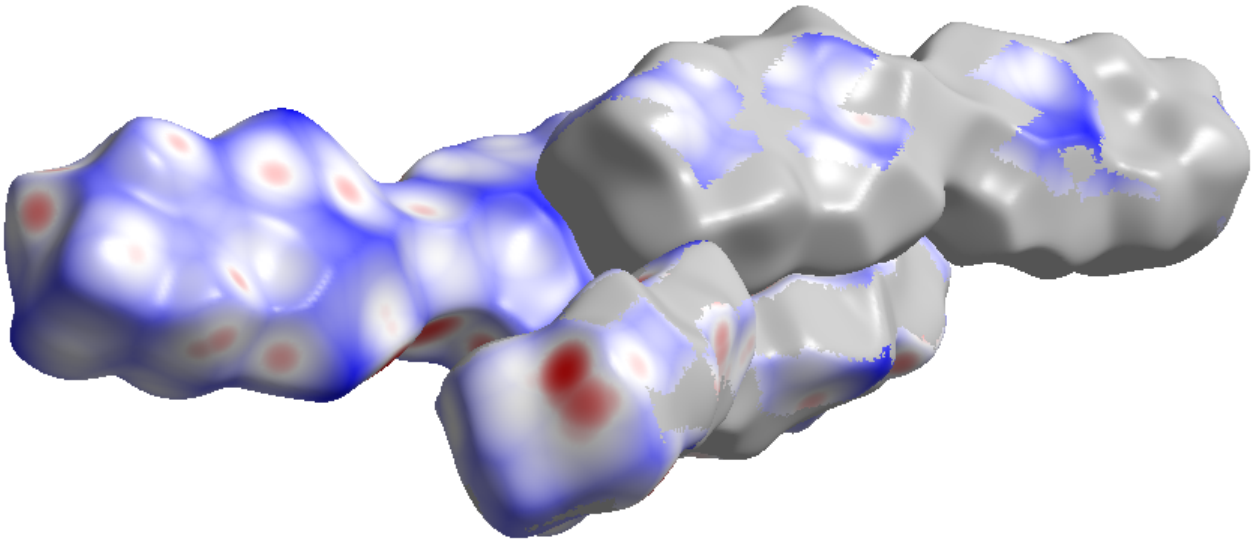

*Figure S2. Hirshfeld surface plots of three neighbouring coordination entities in **1** showing different aspects of the intermolecular interactions: Left: Overall interactions, right C…H interactions, and bottom H…H interactions.*

3. Analysis of the Cambridge Structure Database for specific interactions between pyrrolidines and related cyclic molecules.

The Cambridge Structure Database (CSD version 5.35 2013) was searched for organic only fragments according to Figure S2 right. Only error free structures with r-values less than 10% were retained.

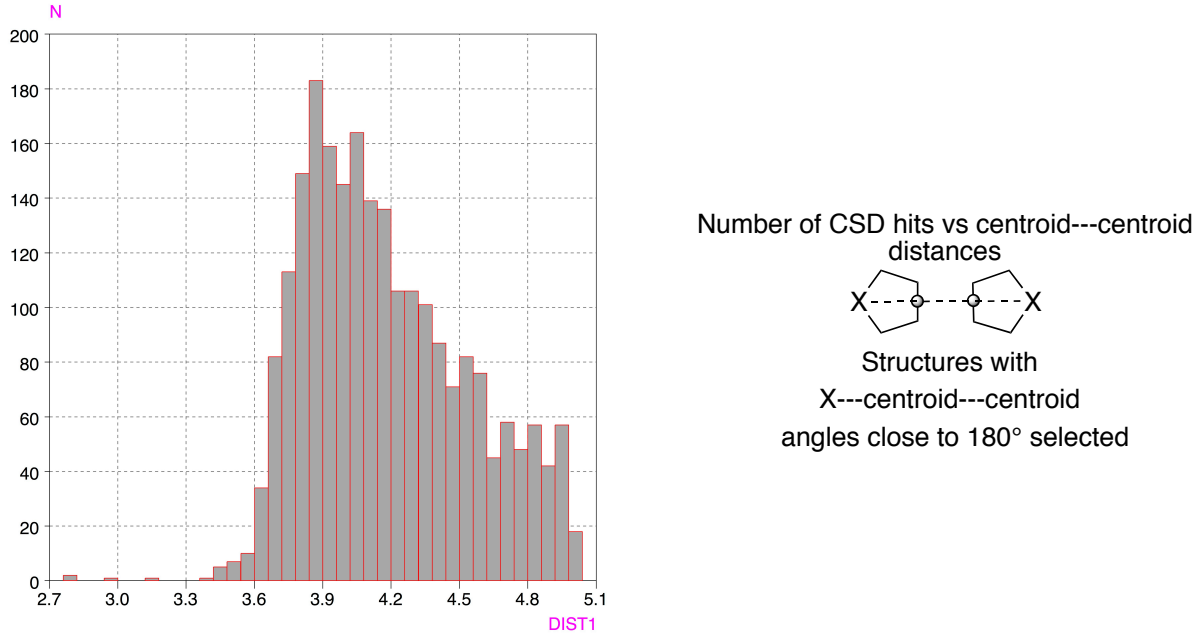

Figure S2.Left: Number of hits plotted against centroid-centroid distances. Right: search fragment and geometry definitions.

4. Experimental Details

The Infrared spectra were recorded on a Brucker IFS-125 model FT-IR spectrophotometer as KBr pellets in the range of 200-4000 cm-1. Thermal analysis is performed in the MicroanalyticalCenter at Cairo University. The thermal analysis of the studied compound has been carried out using a Shimadzu thermogravimetricanalyzer TGA-50H.

[Ag(4-(1-pyrrolidinyl)pyridine)$_2$]NO_3·½H_2O 1was prepared by mixing (0.17 g, 1.0 mmol) 10 ml of an aqueous $AgNO_3$ (0.17 g, 1.0 mmol) and 15 ml of an ethanolic solution containing 4-pyrollidinopyridine (0.15 g, 1.0 mmol), and stirring the solution well for few minutes. It was kept at ambient temperature in a dark place and after two days, colourless long needles were obtained. The crystals were filtered off and washed with 1:10 water ethanol solution then air dried to give: 0.20 g, 88% with respect to the ligand. Analytical data (%): Calc.: C, 46.35; H, 5.15; N, 9.01; Ag, 23.18. Found: C, 46.52; H, 5.12; N, 8.99; Ag, 23.31.

[Ag(4-(1-pyrrolidinyl)pyridine)$_2$]ClO_4 3 The compound was prepared by mixing 0.23 g (1.0 mmol) of $AgClO_4$·H_2O in 15 ml of distilled water and 30 ml of an ethanolic solution containing 4-pyrollidinopyridine (0.3 g, 2.0 mmol). The resulting slightly turbid solution was filtered and then kept at ambient temperature in a refrigerator at 8 °C. After three days colourless block-shaped crystals were obtained, filtered off and washed with 1:1 water-ethanol solution and then air dried to give: 0.12 g, 24 % with respect to the silver perchlorate.

X-ray Crystallography All relevant crystallographic data as well as selected interatomic distances and bond angles can be found in the Supplementary Material and the crystallographic data are also available from the CCDC, 12 Union Road, Cambridge CB2 1EZ, UK upon request, quoting the deposition numbers CCDC 1058723 – 1058725. These data can also be obtained at: http://www.ccdc.cam.ac.uk/Community/Requestastructure/Pages/DataRequest.aspx or fax: (internat.) +44-1223-336-033; E-mail: deposit@ccdc.cam.ac.uk.

Antimicrobial activities of the studied compound were determined according to the recommendations of NCCLS40[8] by the use of broth micro-dilution method. Minimum inhibitory concentrations (MICs) for the tested compound were conducted using ten clinical isolates from diabetic foot ulcers (Department of Vascular Surgery, Faculty of Medicine, Alexandria University, Alexandria, Egypt), *M. luteus*, *S. aureus*, and *S. pyogenes*, as Gram-positive bacteria, *E. coli*, *K. pneumoniae*, *Ps. Aeruginosa*, *P. mirabilis*, *E. cloacae*, and *S. enterica* as Gram negative bacteria, and the yeast *C. albicans*. We also tested against the following standard bacteria from the American Type Culture Collection (ATCC). *S. lutea*, ATCC 10031, *S. aureus*, ATCC 6538p, *E. coli*, ATCC 8739 and *Ps. Aeruginosa*, ATCC 9027. The test materials were dissolved in DMSO. The test material were dissolved in DMSO to give a stock solution that was subsequently diluted in the growth medium to give a final concentrations of 256, 128, 64, 32, 16, 8, 2, 1, and 0.5 µg complex /ml. A final concentration of 5% DMSO was present in all assays, a concentration which had no antibacterial effect on its own (a control treatment, with all the tested bacteria, using 10% DMSO showed no antibacterial activity). Bacteria were cultured in Mueller Hinton Broth (MHB) for 24 h at 35°C. MIC values correspond to the lowest concentration that inhibited the bacterial growth.

*5. Crystallography data and additional structure analysis of **1-3***

Table S1 Crystal data and structure refinement for $Ag(L_2)NO_3 \cdot 1/2H_2O$, 4-(1-pyrrolidinyl)-pyridine (Ligand L; **2**), and $Ag(L_2)ClO_4$ **3**.

Compound	(1)	(2)	(3)
Empirical formula	$C_{108}H_{150}Ag_6N_{30}O_{21}$	$C_9H_{12}N_2$	$C_{18}H_{24}AgClN_4O_4$
Formula weight	2851.75	148.21	503.73
Temperature	100(2) K	100(2) K	100(2) K
Wavelength	0.71073 Å	0.71073 Å	0.71073 Å
Crystal system	tetragonal	orthorhombic	monoclinic
Space group	I 4_1	P b c a	P 2_1 / c
Unit cell dimensions	a = 24.5154(14) Å	a = 10.4951(7) Å	a = 11.3787(10) Å
	b = 24.5154(14) Å	b = 8.1040(5) Å	b = 8.1171(7) Å
	c = 76.118(4) Å	c = 18.3689(11) Å	c = 21.410(2) Å
	α= 90°	α= 90°	α= 90°
	β= 90°	β= 90°	β= 95.969(6)°
	γ= 90°	γ = 90°	γ= 90°
Volume	45747(5) $Å^3$	1562.32(17) $Å^3$	1966.8(3) $Å^3$
Z	16	8	4
Density (calculated)	1.653 Mg/m^3	1.260 Mg/m^3	1.701 Mg/m^3
Absorption coefficient	1.090 mm^{-1}	0.077 mm^{-1}	1.193 mm^{-1}
F(000)	23328	640	1024
Crystal size	0.49 x 0.12 x 0.11 mm^3	0.40 x 0.28 x 0.28 mm^3	0.35 x 0.25 x 0.20 mm^3
Theta range for data collection	1.07 to 26.00°	2.95 to 28.49°	2.49 to 24.52
Index ranges	$-30 \le h \le 29$	$-14 \le h \le 14$	$-13 \le h \le 13$
	$-28 \le k \le 30$	$-10 \le k \le 10$	$-10 \le k \le 10$
	$-93 \le l \le 88$	$-24 \le l \le 19$	$-25 \le l \le 26$
Reflections collected	171055	20545	30483
Independent reflections	42838 [R(int) = 0.0332]	1977 [R(int) = 0.0280]	3834 [R(int) = 0.110]
Completeness theta / %	26.0 / 99.7 %	28.49° / 99.9 %	26.0 / 99.5 %
Absorption correction	Semi-empirical from equivalents	Semi-empirical from equivalents	Semi-empirical from equivalents
Max. and min. transmission	0.8895 and 0.6189	0.9788 and 0.9699	0.7888 and 0.7099
Refinement method	Full-matrix least-squares on F^2	Full-matrix least-squares on F^2	Full-matrix least-squares on F^2
Data / restraints / parameters	42838 / 31 / 3013	1977 / 0 / 101	3834 / 0 / 257
Goodness-of-fit on F^2	1.019	1.070	1.017
Final R indices [I>2sigma(I)]	R1 = 0.0357, wR2 = 0.0693	R1 = 0.0369, wR2 = 0.0930	R1 = 0.0488, wR2 = 0.1060
R indices (all data)	R1 = 0.0487, wR2 = 0.0739	R1 = 0.0439, wR2 = 0.1006	R1 = 0.0920, wR2 = 0.1250
Extinction coefficient	---	0.0053(11)	0.0005(3)
Absolute structure parameter	0.00(1)	---	---
Largest diff. peak and hole	0.941 and -1.420 $e.Å^{-3}$	0.342 and -0.178 $e.Å^{-3}$	1.163 and -0.856 $e.Å^{-3}$

Crystal structure of 1

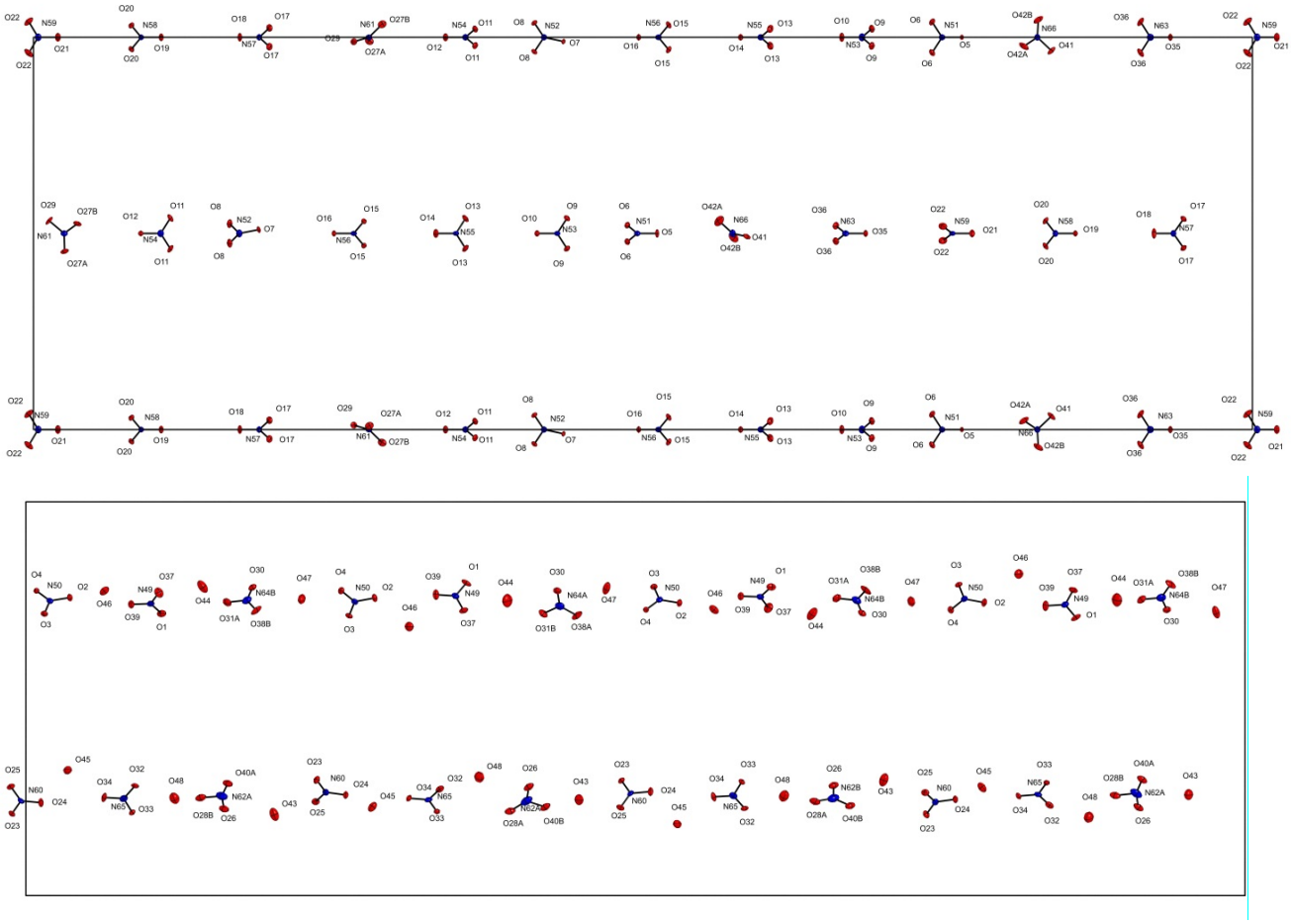

Figure S3. Arrangement of the bonding nitrate ions in the [(AgL$_2$)$_2$NO$_3$] complex units (upper part) and of the non-coordinating nitrates within the channels of the structure (lower part). The long distances of the latter to their respective silver cations of approximately 3.2 – 3.9 Å are compensated by hydrogen bonds to the inserted crystal water, thus leading to chains of alternating nitrate ions and crystal water molecules. For this drawing all silver atoms and organic ligand molecules have been omitted, the structure is shown in a view along [100].

Crystal Structure of the 4-(1-pyrrolidinyl)pyridine ligand, **2**

The crystal structure of the compound 4-(1-pyrrolidinyl)pyridine was determined for a better understanding of the complicated structure of its silver complex. It crystallizes with orthorhombic symmetry in the space group Pbca. The atomic numbering scheme as well as the packing of the ligand molecules in the unit cell is illustrated in the figures S4 and S5, respectively.

Table S2 contains the complete list of interatomic distances occurring in the crystal structure of 4-pyrrolidinopyridine

Table S2. Bond lengths [Å] and angles [°] for 4-pyrrolidinopyridine.

N(1)-C(5)	1.3444(14)	C(2)-C(3)	1.4133(14)
N(1)-C(1)	1.3451(14)	C(3)-C(4)	1.4129(13)
N(2)-C(3)	1.3554(12)	C(4)-C(5)	1.3837(13)
N(2)-C(9)	1.4646(13)	C(6)-C(7)	1.5290(15)
N(2)-C(6)	1.4660(13)	C(7)-C(8)	1.5326(16)
C(1)-C(2)	1.3841(14)	C(8)-C(9)	1.5328(14)
C(5)-N(1)-C(1)	114.52(9)	C(4)-C(3)-C(2)	116.04(9)
C(3)-N(2)-C(9)	123.61(8)	C(5)-C(4)-C(3)	119.26(9)
C(3)-N(2)-C(6)	123.51(9)	N(1)-C(5)-C(4)	125.47(10)
C(9)-N(2)-C(6)	112.78(8)	N(2)-C(6)-C(7)	103.15(8)
N(1)-C(1)-C(2)	125.59(10)	C(6)-C(7)-C(8)	103.40(8)
C(1)-C(2)-C(3)	119.11(9)	C(7)-C(8)-C(9)	103.56(8)
N(2)-C(3)-C(4)	121.89(9)	N(2)-C(9)-C(8)	103.37(8)
N(2)-C(3)-C(2)	122.07(9)		

The molecules of 4-(1-pyrrolidinyl)pyridine form more or less co-planar dimers (see Figure S6), held together by H-π interactions between the hydrogen atoms of the pyrrolidine ring and the π-electron system of the pyridine rings and by π-π-stacking interactions between the pyridine rings.

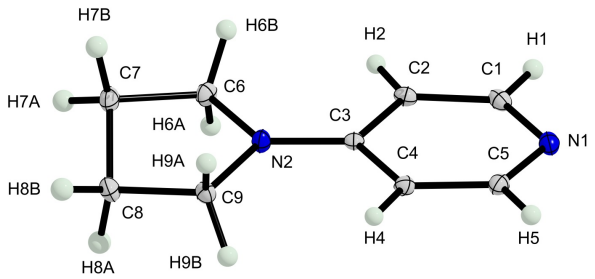

*Figure S4. Structure and atom numbering scheme of the asymmetric unit in compound **2**. All ellipsoids are drawn at the 30 % probability level.*

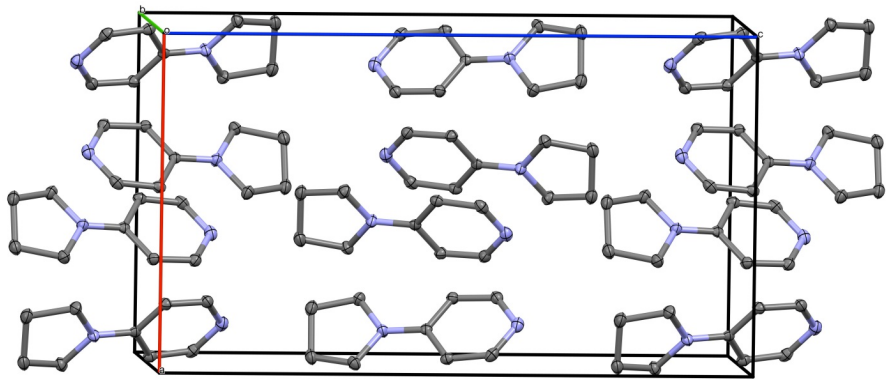

*Figure S5. Unit cell content of compound **2**. The hydrogen atoms are omitted for clarity.*

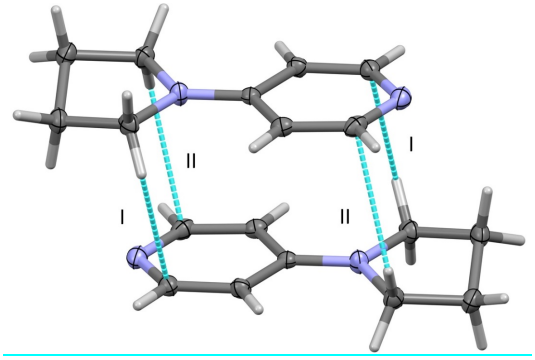

Figure S6. Dimer of 4-(1-pyrrolidinyl)pyridine. The distances I (H6B-C5) and II (H9A-C1) are 2.83 Å and 2.87 Å, respectively.

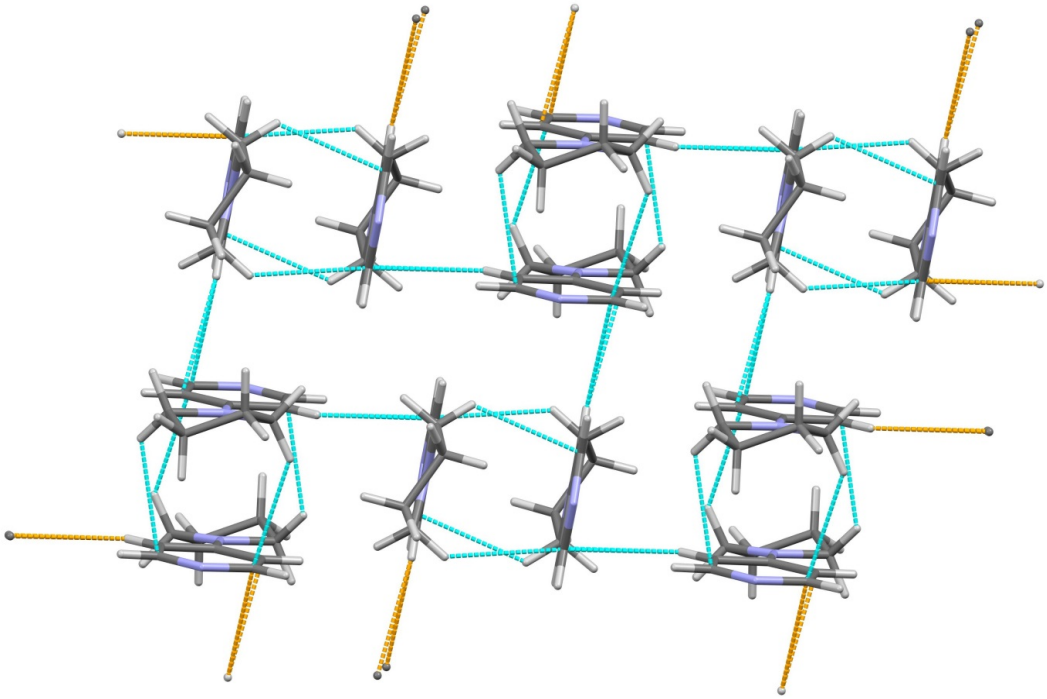

*Figure S7. Packing scheme of the dimeric „sandwiches" in the crystal structure of **2**. The dimers are bonded to another by additional weak H-π-interactions between the hydrogen atoms of the pyridine rings and the π-electron system of the pyridines of the neighbouring "sandwiches", thus forming a 2D-network of primitively packed dimers. These slabs extend parallel to the ab-plane; in the crystallographic c-direction the slabs show only van-der-Waals bonds between the protons of the pyrrolidine rings.*

Furthermore there are also H-π interactions to the neighbouring dimers - arranged perpendicular to the ring planes of the first dimericcomplex as shown in Figure S7.

The crystal structure of free 4-pyrollidinopyridine shows only one type of close interactions between the ligand molecules with each other. The co-planar ring systems overlap in a way that π-π interactions between the aromatic rings as well as H-π interactions between the axial hydrogen atoms of the pyrrolidine rings with the π-electrons of the pyridine rings are possible, while in the complex silver compound a number of different overlap modes can be observed. Anyway, the pure ligand as well as the ligand molecules in the complex structure show a linear overlap along the long axis of the molecules.

A thermal ellipsoid pot of compound **3** [Ag(4-(pyrrolidin-1-yl)pyridine)$_2$]ClO_4 can be found in Figure S8. The Ag1 and Ag2 atoms lie on independent inversion centres.

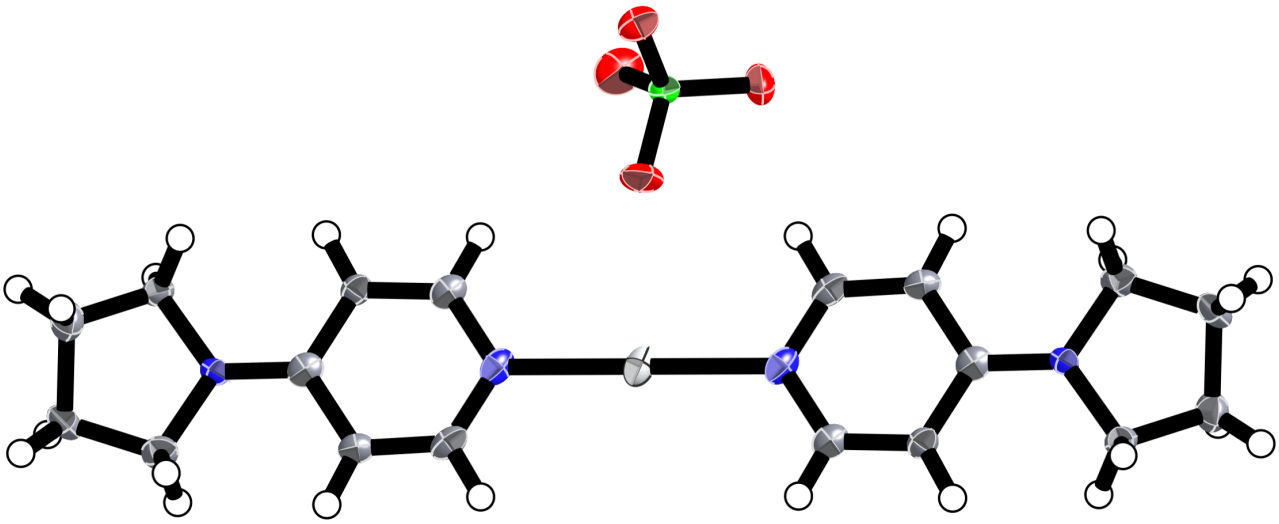

*Figure S8. Thermal ellipsoid plot of a part of the structure of compound **3** [Ag(4-(pyrrolidin-1-yl)pyridine)$_2$]ClO_4. Note that the asymmetric unit has one perchlorate ion and two independent AgL moieties (with the half-occupancy Ag atoms on inversion centres).*

The closest Ag…O distance is 2.97 Å, clearly non-bonding, and the O…H weak hydrogen bonds (C…O 3.35 Å, H…O 2.56 Å and CHO angle 141°) may be more significant. In addition the pyridine rings p-stack on one side, giving a chain zigzag motif, visible in the packing diagram in Figure S9.

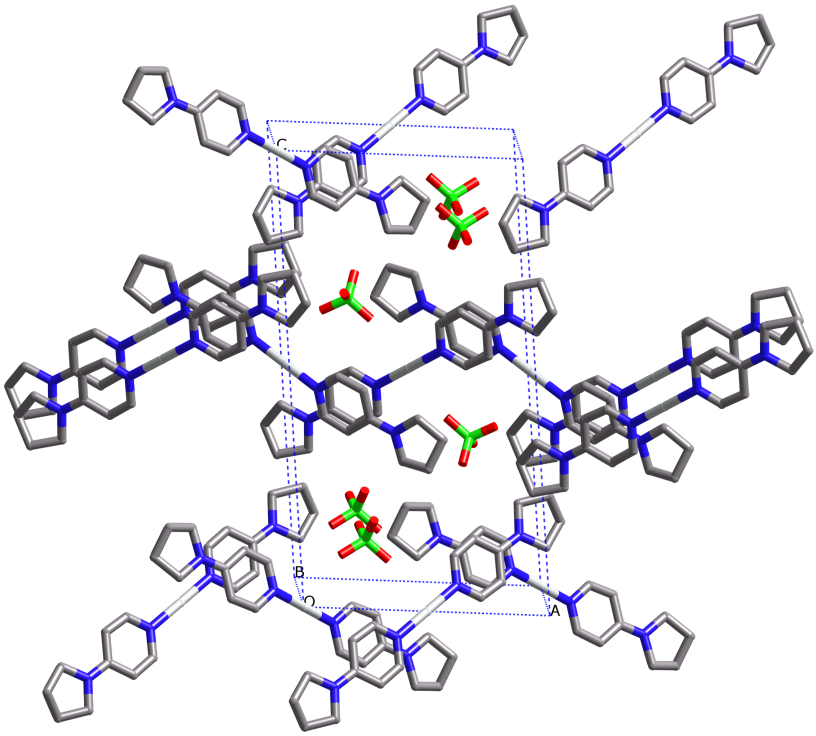

*Figure S9. Packing diagram of compound **3** [Ag(4-(pyrrolidin-1-yl)pyridine)$_2$]ClO_4, hydrogen atoms have been omitted for clarity.*

5. Complete microbial test

Table S1. Minimum inhibitory concentration (MIC) for [Ag(4-(pyrrolidin-1-yl)pyridine)$_2$]NO_3·½H_2O against multi drug resistant diabetic foot bacteria compared with a number of commercial antibiotics. Shaded fields have the lowest MIC for each strain and read fields indicate compound is not active. Roman superscript numbers indicate the generation of the antibiotic. Lower values indicate higher activity.

	Gram-Positive bacteria			**Gram-negative bacteria**							
Antibiotic	***S. lutea*[1]**	***M. luteus*[2]**	***S. aureus*[3]**	***E. coli*[4]**	***K. pneumoniae*[2]**	***Ps. aeruginosa1*[2]**	***Ps. aeruginosa2*[2]**	***Ps. aeruginosa 3*[2]**	***P. mirablis*[2]**	***E. cloacae*[2]**	*C. albicans*[2]
	MIC (µg/ml)										
Amikacin	4	8	4	8	>256	12	32	>256	64	>256	
Gentamicin	16	16	16	4	32	24	24	96	192	>256	
Streptomycin	16	64	12	6	64	16	12	128	128	>256	
Amoxicillin	8	24	8	32	>256	>256	16	192	192	128	
Ampicillin	64	16	4	24	>256	8	8	96	128	96	
Cephradine[i]	48	64	16	24	192	128	32	192	192	>256	
Cefuroxime[ii]	32	32	8	16	128	64	16	128	96	128	
Cefoperazone[ii]	16	16	6	12	96	8	16	96	32	48	
Cefepime[iv]	24	8	4	4	64	32	8	48	24	32	
Imipenem	8	32	2	3	>256	>256	64	96	>256	16	
Meropenem	32	16	2	2	192	128	48	64	128	12	
Azithromycin	16	16	12	12	64	128	64	128	48	64	
Clarithromycin	24	24	16	8	32	96	48	96	32	32	
Nalidixic acid[i]	8	32	24	4	128	64	48	128	>256	>256	
Ciprofloxacin[ii]	4	24	4	6	32	48	24	64	64	128	
Levofloxacin[iii]	16	16	3	8	16	32	16	32	32	32	
Vancomycin	32	24	32	4	128	64	32	128	48	64	
1	16	32	32	32	64	16	32	16	24	32	8

[1]ATCC 10031 [2]Clinical [3]ATCC 6538p, [4]ATCC 8739 [5]ATCC 9027

1 Russo, J., Romano, F. & Tanaka, H. New metastable form of ice and its role in the homogeneous crystallization of water. *Nat Mater***13**, 733-739, doi:10.1038/nmat3977 http://www.nature.com/nmat/journal/v13/n7/abs/nmat3977.html - supplementary-information (2014).
2 Zhao, Z. *et al.* Tetragonal Allotrope of Group 14 Elements. *J. Am. Chem. Soc.***134**, 12362-12365, doi:10.1021/ja304380p (2012).
3 Öhrström, L. & O'Keeffe, M. Network topology approach to new allotropes of the group 14 elements. *Z. Krist. Cryst. Mat.***228**, 343-346, doi:10.1524/zkri.2013.1620 (2013).
4 Delgado-Friedrichs, O. & O'Keeffe, M. Identification and symmetry computation for crystal nets. *Acta Cryst. Sec. A***59**, 351-360 (2003).
5 Blatov, V. A., O'Keeffe, M. & Proserpio, D. M. Vertex-, face-, point-, Schlafli-, and Delaney-symbols in nets, polyhedra and tilings: recommended terminology. *CrystEngComm***12**, 44-48, doi:10.1039/b910671e (2010).
6 O'Keeffe, M., Peskov, M. A., Ramsden, S. & Yaghi, O. M. The Reticular Chemistry Structure Resource (RCSR) Database of, and Symbols for, CrystalNets. *Acc. Chem. Res.***41**, 1782-1789 (2008).
7 O'Keeffe, M. New ice outdoes related nets in smallest ring size. *Nature* **392**, 879 (1998).
8 Performance standards for antimicrobial susceptibility testing. NCCLS approved standard M100-S9.; National Committee for Clinical Laboratory Standards (NCCLS): Wayne, PA, 1999.